Magma Evolution and Mantle Metasomatism: Constraints on Olivine Composition in Potassic-Ultrapotassic Mafic Rocks from Lar Igneous Suite, SE of Iran

S. Ghafaribijar[*], M. Arvin, S. Dargahi

Department of Geology, Faculty of Sciences, University of Shahid Bahonar, Kerman, Islamic Republic of Iran

Abstract

The Lar igneous suite (LIS), in southeastern Iran, is part of post collisional alkaline magmatism in Sistan suture zone. Shonkinite and kersantite are the only two high-Mg, K-rich olivine bearing rocks in the LIS. We study major and some compatible trace elements in the Lar shonkinite and kersantite (LSK) olivines to define mantle mineralogy and metasomatic processes. Olivines in shonkinite have higher Fo (83-90), compared with those in kersantite (Fo_{76-80}). Ca and Ni contents in the olivines are relatively low, whereas their Mn and Ti contents are high and variable, respectively. Low Ni contents exhibit olivine crystallization at igneous conditions from a magma originated by partial melting of an olivine-rich mantle source. Geochemical date reveal that magma evolution is responsible for high-Mn and low Fo contents in kersantitic olivines. In contrast, high Mn, Mn/Fe and Fo contents in shonkinitic olivines indicate an existence of Mn-rich and Ca-Si-poor metasomatic agents in the source. So, considering the Middle Oligocene-Miocene post-collision nature of the Lar igneous suite, melts or fluids derived from upwelling asthenosphere in the form of magnesitic-carbonatite melts, had great potential in metasomatism of subcontinental lithospheric mantle. This CO_2 and K-rich liquid then reacts with peridotite to produce new mineral assemblages including low-Ca clinopyroxene, olivine and phlogopite. Partial melting of such metasomatized source region was responsible for producing the undersaturated, K-rich shonkinite and kersantite in the LIS.

Keywords: Lar; Kersantite; Shonkinite; Olivine; Mantle Metasomatism.

Introduction

Olivine is the first liquidus silicate phase, which crystallizes from mantle derived mafic magmas, with a liquidus phase field that expands at low-pressures [1-6]. So, the olivine composition in term of major and trace elements has enormous potential for deciphering the nature and evolution of the mantle, its melting history and early crystallization of the resulted magmas [1, 3, 4, 7-11]. Olivine Mg-value (Fo= 100*Mg/(Mg+Fe) is another major compositional factor that provides useful information on the mineralogy of the mantle sources

[1], the composition of primitive mantle derived melts and the fractionation degree of magmas [4, 9]. Olivine composition has been also used to investigate metasomatic processes that involved in the generation of mantle derived K-rich rocks, in order to determine the differences between potassic ($K_2O/Na_2O>1$) and common magmas in various tectonic settings [1, 3, 4, 12-15].

In this paper, we present major and some compatible trace elements (such as Ni, Cr, and Mn) in olivines from the Lar shonkinite and kersantite (LSK) rocks that were intruded into the Oligocene volcanic and metamorphic rocks in southeastern Iran. These rocks are high-Mg mafic potassic-ultrapotassic in composition with $K_2O/Na_2O=$ 1.46-2.79; MgO > 3 wt%; and $K_2O > 3$ wt %. By using the olivine composition we proved the role of mantle mineral assemblage, magmatic processes and metasomatic agents in the source region of the LSK rocks in the Lar igneous suite (LIS). We also define, due to alkaline and silica-undersaturated nature of the LSK rocks along with high Mn and Mn/Fe ratio and low Ca

and Ni contents in olivine, that the olivine grains in the LSK rocks are igneous and crystallised from a magma which has been originated by partial melting of a mantle source metasomatized by magnesitic-carbonatite melts, rather than partial melting of a refractory mantle source.

Geological setting and geology of the area

As a part of the Alpine–Himalayan orogenic system and Gondwana-derived continental blocks, Iran accreted to the southern margin of Eurasia following the subduction of Neotethys oceanic crust during the Late Paleozoic to Early Mesozoic [16]. This led to the development of three mountain ranges in Iran: (a) Alborz–Kopeh Dagh in the north, (b) Zagros orogenic belt in the southwest and (c) East Iranian ranges in the east (Fig. 1a; [17]). They are marked respectively by the Paleotethyan suture, Neotethyan suture and the Sistan suture [16, 18, 19, 20, 21]. The latter named after Sistan oceanic back-arc basin that was one of the multi-branches of Neotethys oceanic basins and closed during Late Cretaceous to Middle Eocene [20, 22]. Its post-
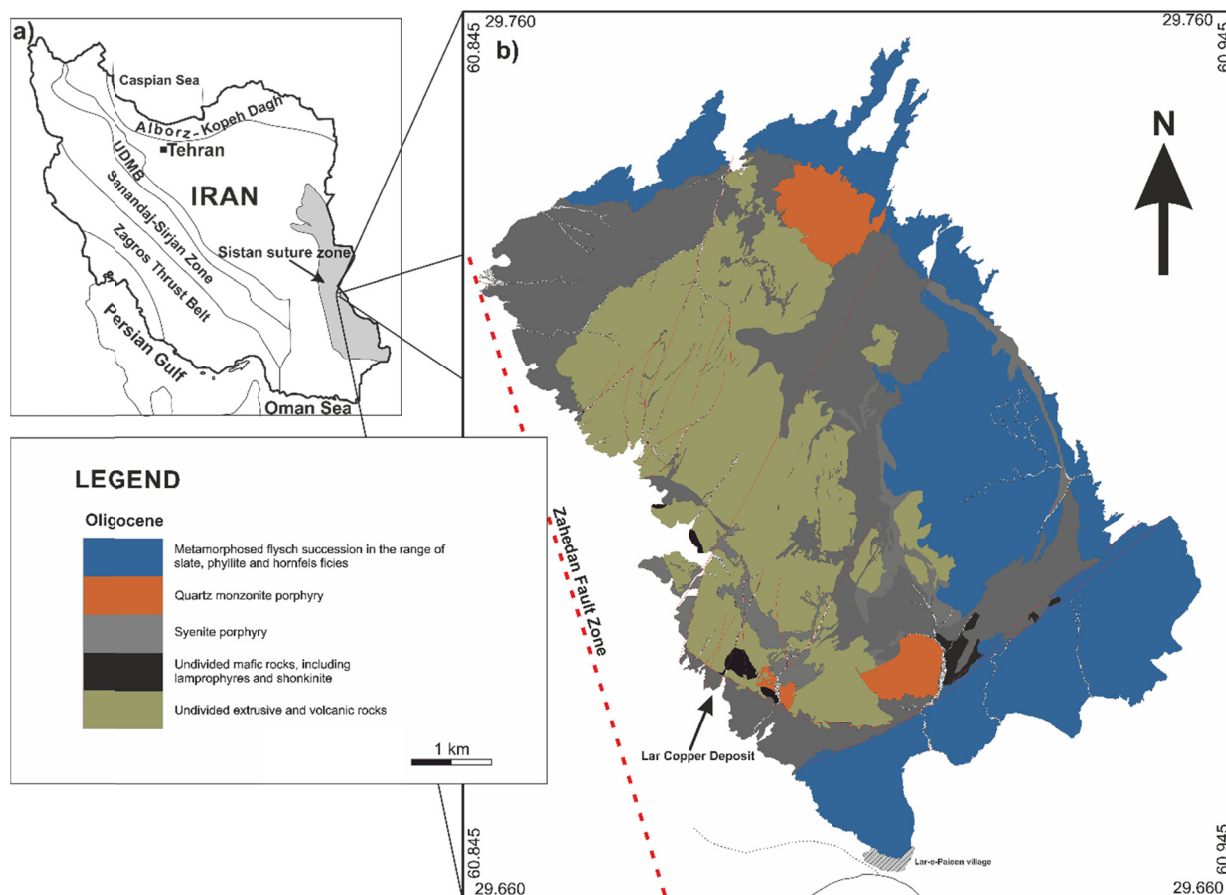
Figure 1. Simple geological map of Lar igneous suite (LIS), showing its important lithological and structural elements, in the Sistan suture zone of southeastern Iran. UDMB: Urmieh-Dokhtar Magmatic Belt.

collision era in the Middle Oligocene-Miocene is marked by emplacement of calc-alkaline Zahedan granite and alkaline igneous complexes such Lar igneous suite (LIS) [23, 24].

The LIS with a northwest trend is located 22 km north of Zahedan in eastern Iran (Fig.1a). The suite comprises of silica-undersaturated to nearly over-saturated intrusive-hypabyssal rock types (kersantite, shonkinite, syenite, monzonite, and nepheline syenite), tuffs and breccias. They are exposed as a series of stocks, dykes, sills, volcanic vents, lava flows and pyroclastics. The shonkinite and kersantite with uneven shape and irregular margins are the two mafic potassic-ultrapotassic rocks that crops out mainly as volcanic vents and sill-like hypabyssal units (with variable width and length) in between syenitic dike and metamorphosed flysch (Fig. 1b).

Materials and Methods

Olivine in representative samples of kersantites and shonkinites were selected for analyses, using Cameca SX-50 electron microprobe in the Department of Earth, Ocean and Atmospheric Sciences at the University of British Columbia in Canada. The olivine composition is determined with standard program: beam current of 20 nA, an acceleration voltage of 15 kV with peak counting times of 20 seconds. Off-peak background counts were collected for 10 seconds. A standard beam 2–5 µm in diameter was used for the analysis of olivine. Natural and synthetic minerals as Standard sets were used.

Results and Discussions
Petrography

In the LIS, kersantite (calc-alkaline lamprophyre) and shonkinite (melanocratic nepheline syenite) are the only mafic rocks that contain olivine. Kersantite mainly contains phenocrysts of euhedral to subhedral clinopyroxene and anhedral olivine, set in a fine to medium-grained matrix of lath shape plagioclase, anhedral biotite, and minor k-feldspar grains. Anhedral microphenocrysts of olivine also occur as inclusions in the clinopyroxene phenocrysts and as aggregates in the matrix (Fig. 2a).

Shonkinite mainly consists of olivine, clinopyroxene, nepheline and rarely biotite grains that are poikiliticaly enclosed by K-feldspars oikocrysts (Fig. 2b). The clinopyroxene and olivine occur as euhedral-subhedral and anhedral phenocrysts, respectively. Nepheline occurs as subhedral medium to fine-grained fingerprint-like minerals that probably resulted by the breakdown of leucite minerals [25, 26]. The biotite occurs as rare subhedral to anhedral microcrysts that tangentially attached to other phenocrysts. The infrequent existence of biotite may indicate low contents of OH and F in the magma [27, 28]. Late and anhedral K-feldspars oikocrysts enclosed existing minerals in shonkinite (Fig. 2b). In both shonkinite and kersantite, olivine shows reaction rim and alteration to iddingsite and opaque minerals. In both rock type's apatite and opaque are the most common accessory minerals and clinopyroxene rarely show schillerean structure.
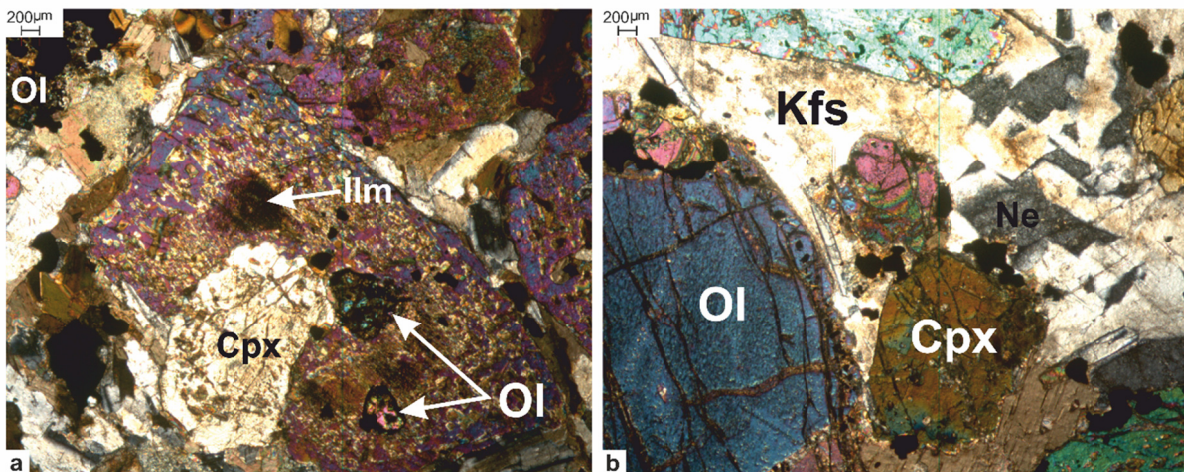
Figure 2. Cross polarized light photomicrographs of kersantite (a) and shonkinite (b) thin sections. Olivine micophenocrystes poikiliticaly enclosed by host clinopyroxene (a), olivine, clinopyroxene and nepheline in a k-feldspar oikocrysts (b). Bio: biotite, Cpx: clinopyroxene, Ilm: ilmenite, Kfs: K-feldspar, Ne: nepheline, Ol: olivine. Abbreviation based on Whitney and Evans, [45].

Olivine major and minor element compositions

The results of olivine phenocrysts (core, mantle and rim) and microphenocrysts (core and rim) analyses in the LSK are given in Table 1. It has been argued that the forsterite (Fo) content of olivine is commonly attributed to magma fractional crystallization [29]. Olivine grains in the LSK are not primitive (Fo<93) and display nearly large range of Fo compositional variations, with Fo_{76-80} in kersantite and Fo_{83-90} in shonkinite. So, the olivine in kersantite is distinctly more evolved than those in shonkinite. Noteworthy, olivine as rare inclusion in host clinopyroxene in kersantite shows high content of forsterite (Fo_{80}); which may point to their preservation from further differentiation effects.

Table 1. Representative electron microprobe analyses of olivines in the Lar shonkinite and kersantite rocks. Micro inp: Microphenocryst of olivine in pyroxene. Number of ions on the basis of 4 oxygens.

Sample	Shonkinite	Shonkinite	Shonkinite	Shonkinite	Shonkinite	Shonkinite	Shonkinite	Shonkinite	Shonkinite	Shonkinite
Type		Phenocryst		Microcryst		Phenocryst		Microcryst	Microcryst	
Analysis	1			2	3			4	5	
	core	mantle	rim	core	core	mantle	rim	core	core	rim
MgO	47/65	47/85	46/65	44/78	46/92	46/47	46/87	46/36	46/68	46/64
SiO2	40/58	40/75	40/80	39/73	40/64	40/06	39/95	40/32	40/37	39/87
CaO	0/01	0/05	0/04	0/06	0/09	0/40	0/00	0/06	0/04	0/03
MnO	0/44	0/39	0/46	0/60	0/46	0/46	0/54	0/48	0/41	0/48
Al2O3	0/03	0/03	0/00	0/01	0/03	0/04	0/00	0/00	0/02	0/01
TiO2	0/01	0/02	0/00	0/04	0/02	0/00	0/02	0/00	0/02	0/00
Cr2O3	0/02	0/00	0/00	0/01	0/00	0/01	0/00	0/00	0/02	0/01
FeO	11/56	12/24	12/09	15/65	12/79	12/57	12/86	12/99	12/53	13/02
NiO	0/16	0/18	0/17	0/17	0/21	0/17	0/23	0/22	0/17	0/18
Na2O	0/03	0/11	0/07	0/08	0/08	0/08	0/06	0/07	0/07	0/11
Sum	100/49	101/62	100/29	101/12	101/24	100/27	100/54	100/50	100/33	100/34
Mg	1/749	1/743	1/718	1/667	1/720	1/721	1/733	1/714	1/724	1/729
Si	0/999	0/996	1/008	0/993	0/999	0/995	0/991	1/000	1/000	0/992
Ca	0/000	0/001	0/001	0/001	0/002	0/011	0/000	0/001	0/001	0/001
Mn	0/009	0/008	0/010	0/013	0/010	0/010	0/011	0/010	0/009	0/010
Al	0/000	0/000	0/000	0/000	0/000	0/001	0/000	0/000	0/000	0/000
Ti	0/000	0/000	0/000	0/001	0/000	0/000	0/000	0/000	0/000	0/000
Cr	0/000	0/000	0/000	0/000	0/000	0/000	0/000	0/000	0/000	0/000
Fe	0/238	0/250	0/250	0/327	0/263	0/261	0/267	0/269	0/260	0/271
Ni	0/003	0/003	0/003	0/003	0/004	0/003	0/005	0/004	0/003	0/004
Na	0/001	0/003	0/002	0/002	0/002	0/002	0/001	0/002	0/002	0/003
Sum	3/000	3/004	2/993	3/007	3/001	3/004	3/009	3/001	2/999	3/009
Mg#	0/880	0/875	0/873	0/836	0/867	0/868	0/867	0/864	0/869	0/865
Fo	87/60	87/05	86/83	83/01	86/21	85/94	86/17	85/91	86/50	85/99
Sample	Shonkinite	Shonkinite	Shonkinite	Shonkinite	Shonkinite	Shonkinite	Shonkinite	Shonkinite	Shonkinite	Shonkinite
Type		Phenocryst		micro inp		Phenocryst		Microcryst	Microcryst	
Analysis	6			7	8			9	10	
	core	mantle	rim	core	core	mantle	rim	core	core	rim
MgO	50/06	49/25	48/99	49/51	49/68	49/85	49/57	49/36	49/65	49/53
SiO2	41/55	41/36	40/57	40/61	41/10	40/95	40/72	40/66	41/38	40/61
CaO	0/09	0/10	0/06	0/09	0/09	0/07	0/08	0/07	0/28	0/07
MnO	0/41	0/41	0/38	0/39	0/44	0/38	0/40	0/38	0/39	0/38
Al2O3	0/02	0/02	0/01	0/04	0/07	0/01	0/02	0/04	0/03	0/02
TiO2	0/02	0/01	0/01	0/00	0/03	0/00	0/01	0/02	0/00	0/00
Cr2O3	0/00	0/01	0/02	0/00	0/01	0/01	0/01	0/00	0/01	0/01
FeO	9/47	9/36	9/39	9/68	9/37	9/45	9/35	9/82	9/12	9/17
NiO	0/18	0/15	0/17	0/19	0/22	0/22	0/16	0/26	0/26	0/18
Na2O	0/15	0/09	0/12	0/10	0/08	0/06	0/07	0/10	0/10	0/11
Sum	101/96	100/75	99/71	100/61	101/08	101/00	100/39	100/70	101/21	100/09
Mg	1/794	1/784	1/796	1/802	1/796	1/804	1/804	1/796	1/790	1/808
Si	0/999	1/005	0/998	0/991	0/997	0/994	0/994	0/993	1/001	0/994
Ca	0/002	0/003	0/002	0/002	0/002	0/002	0/002	0/002	0/007	0/002
Mn	0/008	0/008	0/008	0/008	0/009	0/008	0/008	0/008	0/008	0/008
Al	0/000	0/000	0/000	0/001	0/001	0/000	0/000	0/001	0/000	0/000
Ti	0/000	0/000	0/000	0/000	0/000	0/000	0/000	0/000	0/000	0/000
Cr	0/000	0/000	0/000	0/000	0/000	0/000	0/000	0/000	0/000	0/000
Fe	0/190	0/190	0/193	0/198	0/190	0/192	0/191	0/200	0/184	0/188
Ni	0/004	0/003	0/003	0/004	0/004	0/004	0/003	0/005	0/005	0/004
Na	0/003	0/002	0/003	0/002	0/002	0/001	0/002	0/002	0/002	0/003
Sum	3/002	2/995	3/003	3/008	3/002	3/006	3/005	3/007	2/999	3/006
Mg#	0/904	0/904	0/903	0/901	0/904	0/904	0/904	0/900	0/907	0/906
Fo	89/92	89/87	89/87	89/65	89/92	89/95	89/96	89/52	89/97	90/15

Table 1. Ctd

Sample	Shonkinite	Shonkinite	Shonkinite	Shonkinite	Shonkinite	Shonkinite	Shonkinite	Shonkinite	Kersantite	Kersantite
Type	Microcryst			Phenocryst		Microcryst	Microcryst		Microcryst	
Analysis	11		12			13	14		15	
	core	rim	core	mantle	rim	core	core	rim	core	rim
MgO	48/12	49/62	49/99	49/07	49/43	49/31	49/73	49/50	42/11	41/86
SiO2	40/79	40/90	41/08	40/20	40/96	40/38	40/67	41/06	38/05	39/18
CaO	0/84	0/12	0/07	0/32	0/03	0/08	0/12	0/10	0/02	0/04
MnO	0/33	0/43	0/38	0/31	0/40	0/50	0/34	0/41	0/74	0/78
Al2O3	0/06	0/02	0/00	0/03	0/01	0/02	0/02	0/04	0/01	0/03
TiO2	0/01	0/00	0/00	0/00	0/01	0/00	0/02	0/03	0/00	0/00
Cr2O3	0/00	0/00	0/00	0/00	0/00	0/06	0/01	0/00	0/01	0/00
FeO	10/17	9/59	9/25	9/68	9/60	9/53	9/19	9/56	18/22	18/18
NiO	0/14	0/14	0/22	0/16	0/15	0/17	0/14	0/21	0/04	0/12
Na2O	0/11	0/04	0/06	0/09	0/06	0/08	0/08	0/07	0/08	0/10
Sum	100/56	100/86	101/06	99/86	100/64	100/13	100/30	100/99	99/28	100/29
Mg	1/757	1/799	1/806	1/801	1/795	1/804	1/811	1/792	1/621	1/591
Si	0/999	0/995	0/996	0/990	0/998	0/991	0/993	0/997	0/983	0/999
Ca	0/022	0/003	0/002	0/009	0/001	0/002	0/003	0/003	0/000	0/001
Mn	0/007	0/009	0/008	0/006	0/008	0/010	0/007	0/008	0/016	0/017
Al	0/001	0/000	0/000	0/000	0/000	0/000	0/000	0/000	0/000	0/000
Ti	0/000	0/000	0/000	0/000	0/000	0/000	0/000	0/001	0/000	0/000
Cr	0/000	0/000	0/000	0/000	0/000	0/000	0/000	0/000	0/000	0/000
Fe	0/208	0/195	0/187	0/199	0/196	0/196	0/188	0/194	0/394	0/388
Ni	0/003	0/003	0/004	0/003	0/003	0/003	0/003	0/004	0/001	0/003
Na	0/003	0/001	0/001	0/002	0/001	0/002	0/002	0/002	0/002	0/002
Sum	3/000	3/005	3/005	3/010	3/002	3/009	3/007	3/002	3/018	3/001
Mg#	0/894	0/902	0/906	0/900	0/902	0/902	0/906	0/902	0/805	0/804
Fo	88/11	89/68	90/16	89/37	89/77	89/66	90/16	89/72	79/80	79/68

Sample	Kersantite	Kersantite	Kersantite	Kersantite	Kersantite	Kersantite	Kersantite	Kersantite
Type		Phenocryst		Microcryst	micro inp	Microcryst	Microcryst	
Analysis	16			17	18	19	20	
	core	mantle	rim	core	core	core	core	rim
MgO	41/58	41/92	41/36	40/56	41/82	40/54	40/41	39/29
SiO2	39/13	39/51	38/24	38/83	38/16	38/49	38/47	37/57
CaO	0/01	0/01	0/06	0/01	0/04	0/02	0/01	0/01
MnO	0/72	0/78	0/79	0/84	0/73	0/63	0/61	0/73
Al2O3	0/00	0/02	0/02	0/00	0/00	0/02	0/03	0/03
TiO2	0/00	0/00	0/00	0/03	0/01	0/00	0/00	0/00
Cr2O3	0/00	0/05	0/04	0/00	0/01	0/01	0/01	0/03
FeO	18/47	18/23	19/10	19/86	17/91	20/29	20/56	21/51
NiO	0/07	0/04	0/05	0/10	0/08	0/13	0/09	0/13
Na2O	0/05	0/05	0/07	0/07	0/01	0/09	0/09	0/00
Sum	100/04	100/61	99/72	100/29	98/78	100/22	100/28	99/31
Mg	1/585	1/587	1/591	1/554	1/615	1/558	1/554	1/536
Si	1/001	1/003	0/987	0/998	0/989	0/993	0/992	0/985
Ca	0/000	0/000	0/002	0/000	0/001	0/000	0/000	0/000
Mn	0/016	0/017	0/017	0/018	0/016	0/014	0/013	0/016
Al	0/000	0/000	0/000	0/000	0/000	0/000	0/000	0/000
Ti	0/000	0/000	0/000	0/001	0/000	0/000	0/000	0/000
Cr	0/000	0/000	0/000	0/000	0/000	0/000	0/000	0/000
Fe	0/395	0/387	0/412	0/427	0/388	0/438	0/444	0/472
Ni	0/001	0/001	0/001	0/002	0/002	0/003	0/002	0/003
Na	0/001	0/001	0/002	0/002	0/000	0/002	0/002	0/000
Sum	3/000	2/996	3/013	3/002	3/011	3/008	3/008	3/013
Mg#	0/801	0/804	0/794	0/785	0/806	0/781	0/778	0/765
Fo	79/41	79/71	78/69	77/72	79/94	77/52	77/27	75/87

Furthermore, the average content of Ca in olivines in the LSK (Ca=694 ppm) is less than those in MORB (Ca=2000ppm) and arc settings (Ca=1000ppm) but slightly higher than those in peridotite xenoliths (Ca=276-233 ppm) [11, 30, 31]. But the average content of Mn in olivines in the LSK (Mn=3895 ppm) is higher than those from mantle-derived rocks (MnO= 0.09-0.17 wt % or Mn= 700-1300 ppm; [3]).

The average concentration of Cr in olivines of kersantite (Cr=110ppm) is almost twice than those in shonkinites (Cr=56ppm) but lower than those in OIB (Cr=~400-700 ppm) and MORB (Cr=~350-550 ppm) [11]. In contrast, the average Ni abundances in olivines of shonkinite (Ni=1457 ppm) is higher than those in kersantite (Ni=663 ppm). Ti and Al concentrations in olivines of shonkinite are 0-240 ppm and 0-361 ppm, respectively. Also, Ti and Al concentrations in olivines of kersantitic rocks are 0-192 ppm and 0-155 ppm,

respectively (Table 1). The lack of any consistency between Ti and Al in olivines of the LSK indicates the absence of any coupled substitution in olivine [32].

Mantle or igneous olivines

The distribution of trace elements such as Ca, Al, Ti and Ni in olivine may also facilitate to distinguish igneous from mantle olivines [4, 33, 34, 35]. The mantle olivines have lower concentrations of Ca (< 700 ppm) and Ti (< 70 ppm) in comparison to igneous one [3, 4], that crystallize at lower pressures, with variable Ca and Ti contents (Fig. 3a). In the diagram of Ca (ppm) versus Ti (ppm) (Fig. 3a), most olivines in the LSK have low Ca but elevated Ti concentrations and plot both in

mantle and igneous field; the samples follow the trend of kimberlites with low Ca and high Ti content that were attributed to metasomatic reactions within the mantle source [3, 4, 8].

The Al content is also believed to be high in igneous olivine, reaching up to 800 ppm in comparison to mantle olivine that have less than 130 ppm [4, 8]. However, Al content in olivines in the LSK is relatively low (Al=0-361 ppm) that has overlap with both mantle and igneous olivines; so, the Al content in LSK olivines cannot be used as a determination factor. While, the Ni content is more useful than other transitional elements to distinguish mantle olivines from igneous ones [3, 4, 8]. On the other hand, olivines crystallized from
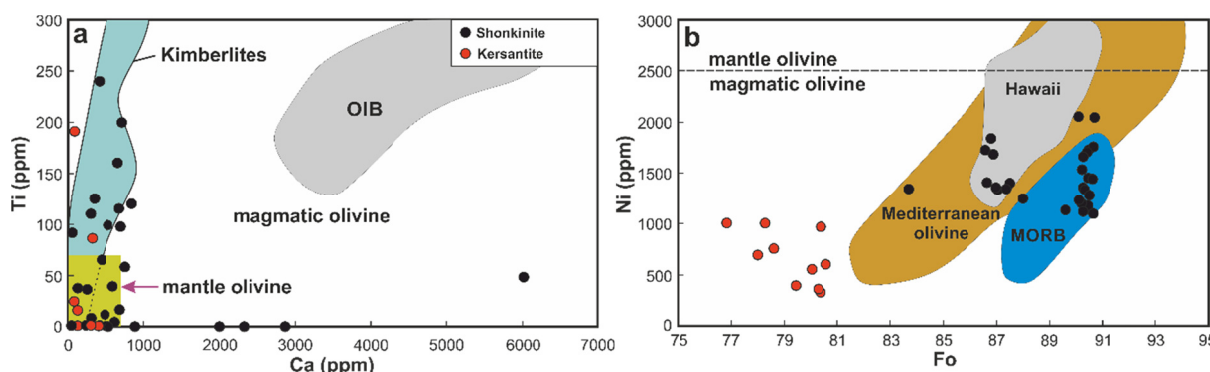
Figure 3. (a) Variation of Ca versus Ti diagram for olivines in the LSK. Mantle peridotite olivine (green box) show restricted ranges for Ti and Ca in comparison to magmatic olivine. (b) Variation of Fo versus Ni diagram for olivines in the LSK. The olivines show lower Ni concentration, in comparison to those from mantle-derived magmas that have Ni concentration within the range of 2500-3100 ppm. These indicate the magmatic origin of olivines in the LSK via crystallization from a more fractionated mafic magma. Data sources for olivines in: kimberlite [8, 41], Hawaii [11], MORB [11], Mediterranean [34], Oceanic island Basalts (OIB)[42]. Field for mantle olivines from Foley et al., [3].
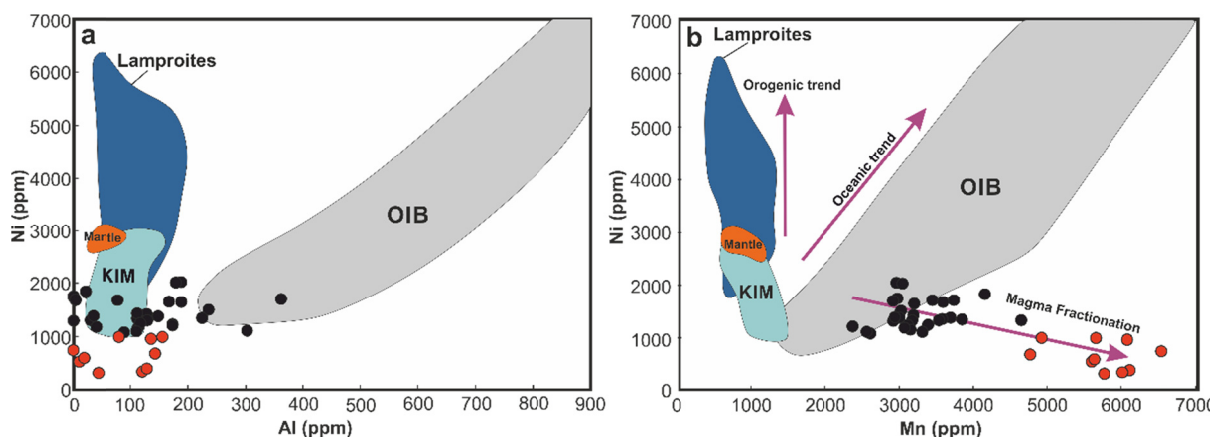
Figure 4. Variation of Al versus Ni (a) and Mn versus Ni (b) diagrams in olivines in the LSK with comparison to kimberlite, lamproite, Ocean Island and mantle olivines (fields after Foley et al., [4]). Arrows show three trends of oceanic, orogenic and magma fractionation that diverge from mantle-like values. Orogenic trend corresponds to continental crust recycling into the mantle in post collision volcanism whereas oceanic trend correlates with recycled oceanic crust. Mn in the LSK show opposite behavior to Ni and reaching high values which is consistent with magma fractionation especially in the case of olivines in kersantite. Data sources: Ocean islands [42], Mediterranean lamproites [34, 43]; kimberlites [8, 41]; mantle olivines (olivine inclusions in diamond) [44]. Symbols as in figure 3a.

primitive mantle-derived melts have Ni content in the range of 2500 to 3100 ppm [3, 4]; those deviating from this range (Fig. 3b) are igneous olivines which crystallized from fractionated melts (lower Ni) or involve partial melting of a pyroxenite source (higher Ni) [3]. In the Fo versus Ni diagram (Fig. 3b), all olivine grains have Ni content lower than 2500 ppm; in this diagram, some olivines in shonkinite have Fo and Ni content similar to MORB; whereas some with lower Fo values show similarities to Hawaiian olivines. In contrast, olivines in kersantite are more evolved and plot close to the Mediterranean field (Fig. 3b). Therefore, the relatively low Ni content in the LSK olivines matches well with igneous olivines that crystallized from a fractionated melt.

Also, olivines in the LSK show a weak and negative correlation between Ni with Al and Mn contents, respectively (Fig. 4a, b). However, Al content in olivines is generally low and stretches into the field of OIB (Fig. 4a). The negative correlation of Ni with Mn in olivines in the LSK (Fig. 4b) indicates igneous fractionation which is characteristic of arc basalts, East African melilitites and some kimberlites [4]. However, fractional crystallization cannot explain the contemporary high Fo and Mn contents in some olivines in shonkinite. This is inconsistent with olivines of high Fo and low Mn contents which are usually crystallize from primary magmas. Therefore, high Fo and Mn contents in some olivines in shonkinite needs a primary source enriched in Mn.

Mantle source and the role of metasomatic agents

Olivine is generally the earliest crystallizing phase in mafic igneous rocks and therefore has the potential to record information about primary melts close to their original, undifferentiated compositions in equilibrium with their mantle source [1]. Olivine phenocrysts then reflect the primary melt compositions. Many authors used Ni, Ca, Mn, Mg and Fe concentrations in olivine to verify its mantle source lithology and the nature of metasomatic agents in the source region [1, 3, 11]. Olivines in the LSK have lower Ca and Ni contents but higher Mn concentration in comparison to olivines of MORB and mantle sources. Nickel content of olivine decreases during fractionation, whereas Ca and Mn contents increase; so the high Mn and low Ca concentrations in olivines of the LSK (especially in shonkinite) cannot be related simply to magmatic fractionation. In order to find out the degree of fractional crystallization in LSK parental melts, the Fo content in olivine has been used. The Fo content of olivines in some shonkinites (Table 1) is similar to those in MORB (Fo_{88-91}; [11]) which argues against high

degree of fractionation. So, the magma fractionation in shonkinite, in contrast to more evolved kersantitic magma, is unlikely to be responsible for high Mn and low Ca and Ni contents in olivine.

Foley et al [3, 4] believe that the low Ca and high Ti contents in olivines are related to a silica-poor metasomatic agent that was enriched in Ti and depleted in Ca. Ammanati et al., [1] showed that there is a relationship between olivine chemistry (especially Ni content) and magma composition in term of SiO_2 content. In contrast to silica saturated magmas, olivines that crystallized from silica-undersaturated magmas, similar to LSK olivines, are depleted in Ni [1]. A general consensus exists among experimental petrologists that phlogopite and K-richterite have great potential to produce silica-undersaturated and silica-oversaturated melts, respectively [36, 37, 38]. Phlogopite and K-richterite are also known from metasomatized mantle assemblages that yield K-rich magmas [12]. The LSK rocks are high-Mg, silica-undersaturated and K-rich rocks which confirm their derivation from a phlogopite-bearing mantle source. Moreover, this silica-undersaturated, phlogopite-and olivine-bearing mantle source requires an interaction between the peridotitic mantle and CO_2-rich metasomatic agents [1].

In the 100*Ca/Fe versus 100*Ni/Mg diagram (Fig. 5) olivines in the LSK are different from those in leucitite, MORB, oceanic Island basalts and lamproites; but their Ni/Mg ratio is low and similar to leucitite. Also, in the 100*Mn/Fe versus 100*Ni/Mg diagram (Fig. 6) olivines in the LSK show similar trends but higher Mn/Fe ratios in comparison to leucitites. The high 100*Mn/Fe ratio of olivines is the characteristic of melts that resulted from strongly depleted peridotite, in which olivine and Cr-rich spinel are residual phases with D_{Mn}/D_{Fe} ratio <1 [4, 39]. Partial melting of such refractory peridotite at higher temperature (in comparison to alkaline magmas) could explain high Mn/Fe ratios of olivines; but is unable to explain high Mn-olivines and high K_2O/Na_2O ratios in the bulk rock composition of the LSK. High Mn/Fe ratio in olivine is also the characteristic of melts that resulted from a mantle source metasomatized by carbonatitic melts [1]. On the other hand, the high Mn/Fe ratios also suggest an increase in the bulk D_{Fe} during melting of a mantle source metasomatized by carbonatitic melts at high pressures [1, 11]. Carbonatitic metasomatism in the mantle will result a high Ca mantle source and high Ca olivine phenocrysts from strongly silica undersaturated rocks [1], which is inconsistent with low Ca content of the LSK olivines; but Rudnick et al., [40] believed that high pressure metasomatism by magnesitic-carbonatite
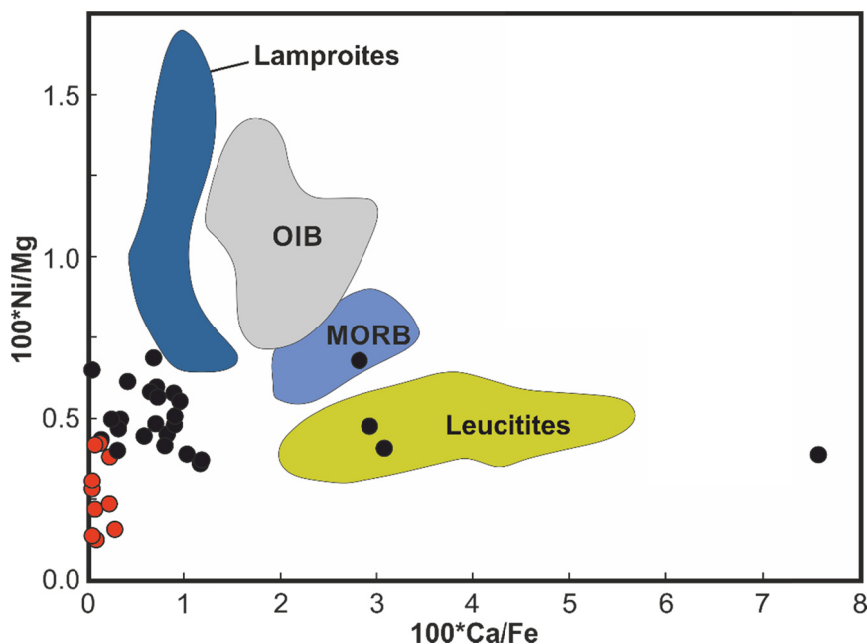
Figure 5. Variation of 100*Ca/Fe versus 100*Ni/Mg diagram for olivines in the LSK (after Ammanati et al., [1]). OIB and lamproitic olivines have high Ni/Mg ratios (crystallized from melts that derived from olivine-free sources with different recycled components). Olivines in Italian leucitites and in the LSK samples show low Ni/Mg and Ca/Fe ratios. Data sources: Ocean islands, MORB, Peridotite, Pyroxenite [11], lamproites and leucitites (Ammanati et al., [1]). Symbols as in figure 3a.
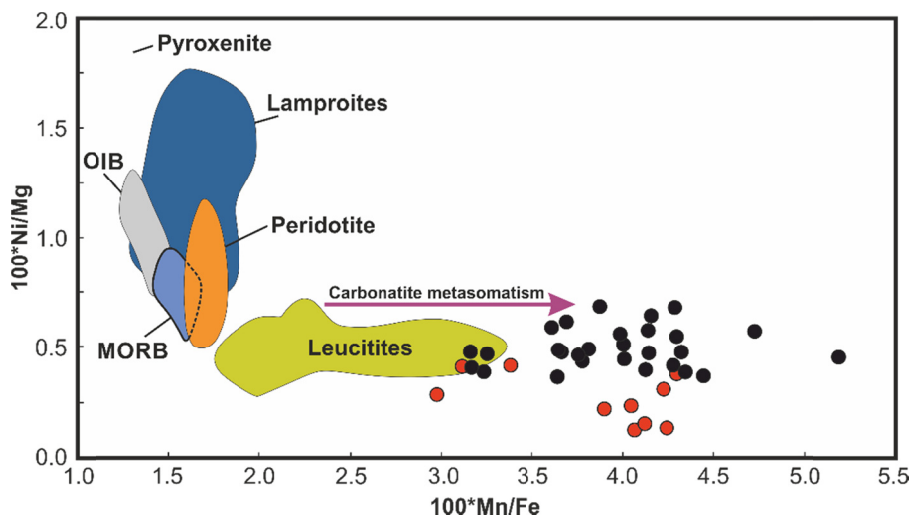
Figure 6. Variation of 100*Mn/Fe versus 100*Ni/Mg ratios in LSK olivines (after Ammanati et al., [1]). Olivines in both OIB and lamproitic are from olivine-free sources, but with different recycled components, have high Ni/Mg ratios. Olivines of Italian leucitites and those from the LSK samples show low Ni/Mg but unusually high Mn/Fe ratios. Data sources: Ocean islands, MORB, Peridotite, Pyroxenite [11], lamproites and leucitites [1]. Symbols as in figure 3a.

melts is responsible for the lack of Ca in mantle. In other words, partial melting of a mantle source metasomatized by magnesitic-carbonatite yields a Ca-poor, Mn-rich magma with high Mn/Fe ratios. Partial melting of this source region is also responsible for the silica-undersaturated, K-rich nature of the LSK rocks. Phlogopite, due to its great potential in generating

silica-undersaturated and K-rich magmas, must be the most important K-rich phase [36, 37, 38]. So, we hereby propose that the LSK rocks most probably originated by partial melting of a mantle source that previously was re-fertilized by magnesitic-carbonatite melts or fluids derived from upwelling asthenosphere. This CO_2 and K-rich metasomatic agent then reacts with surrounding

peridotite to produce new mineral assemblages that include low-Ca clinopyroxene, phlogopite, and olivine.

Geochemical data confirm that olivine grains in most shonkinites have been crystallized from primary silica-undersaturated, K-rich magmas; while olivine grains in kersantite are the result of crystallization from more evolved magmas.

Conclusion

The Lar igneous suite is part of post collisional alkaline magmatism in Sistan suture zone. In this suite kersantite and shonkinite are the only two high-Mg mafic potassic-ultrapotassic rocks that contain olivine grains. Low Ni content in the LSK olivines demonstrate their igneous origin. The low Ni content is also consistent with a mantle source rich in olivine and poor in orthopyroxene. Geochemical data indicate that magma evolution is responsible for extraordinary high Mn content in kersantitic olivines. In contrast, the relatively low Ca, high Mn, Mn/Fe and Fo values in shonkinitic olivines most probably indicates an existence of Mn-rich and Ca-poor metasomatic agent. So, considering the Middle Oligocene-Miocene post-collision nature of the Lar igneous suite, melts or fluids derived from upwelling asthenosphere probably had great potential in metasomatism of subcontinental lithospheric mantle. Low Ca and high Mn/Fe ratio in LSK olivines confirm that this CO_2 and K-rich liquid most probably is a magnesitic-carbonatite magma which reacts with surrounding peridotite to produce new mineral assemblages including low-Ca clinopyroxene, olivine and phlogopite. Partial melting of this source region was responsible for producing the silica-undersaturated, K-rich shonkinite and kersantite in the Lar igneous suite.

Acknowledgments

References

1. Ammannati E, Jacob DE, Avanzinelli R, Foley SF, Conticelli S. Low Ni olivine in silica-undersaturated ultrapotassic igneous rocks as evidence for carbonate metasomatism in the mantle. Earth Planet. Sci. Lett. 2016; 444:64-74.

2. Kushiro I. On the nature of silicate melt and its significance in magma genesis: regularities in the shift of liquidus boundaries involving olivine, pyroxene and silica minerals. Am. J. Sci. 1975; 275:411-431.

3. Foley SF, Jacob DE, O'Neill SC. Trace element variations in olivine phenocrysts from Ugandan potassic rocks as clues to the chemical characteristics of parental magmas. Contrib. Mineral. Petrol. 2011; 162:1-20.

4. Foley SF, Prelevic D, Rehfeldt T, Jacob DE. Minor and trace elements in olivines as probes into early igneous and mantle melting processes. Earth Planet. Sci. Lett. 2013; 363:181-191.

5. Ulmer P, Sweeney RJ. Generation and differentiation of Group II kimberlites: constraints from a high-pressure experimental study to 10 GPa. Geochim. Cosmochim. Acta. 2002; 66:2139-2153.

6. Upton BGJ, Skovgaard AC, McClurg J, Kirstein L, Cheadle M, Emeleus CH, Wadsworth WJ, Fallick AE. Picritic magmas and the Rum ultramafic complex, Scotland. Geol. Mag. 2002; 139:437-452.

7. Green DH, Ringwood AE. The genesis of basaltic magmas. Contrib. Mineral. Petrol. 1967; 15:103-190.

8. De Hoog JCM, Gall L, Cornell D. Trace element geochemistry of mantle olivine and applications to mantle petrogenesis and geo-thermo-barometry. Chem. Geol. 2010;270:196-215.

9. Herzberg C. Identification of source lithology in the Hawaiian and Canary Islands: implications for origins. J. Petrol. 2011;52:113-146.

10. Sobolev AV, Hofmann AW, Sobolev AV, Nikogosian IK. An olivine-free mantle source of Hawaiian shield basalts. Nature. 2005;434:590-597.

11. Sobolev AV, Hofmann AW, Kuzmin DH, Yaxley GM. The amount of recycled crust in sources of mantle-derived melts. Science. 2007;316:412-417.

12. Foley SF, Venturelli G, Green DH, Toscani L. The ultrapotassic rocks: characteristics, classification, and constraints for petrogenetic models. Earth. Sci. Rev. 1987;24:81-134.

13. Chung SL, Wang KL, Crawford AJ, Kamenetsky VS, Chen CH, Lan CY, Chen CH. High-Mg potassic rocks from Taiwan: implications for the genesis of orogenic potassic lavas. Lithos. 2001; 59:153-170.

14. Muller D, Rock NMS, Groves DI. Geochemical discrimination between shoshonitic and potassic volcanic rocks in different tectonic settings: a pilot study. Mineral. Petrol. 1992; 46:259-289.

15. Pang KN, Sun-Lin Chung SL, Zarrinkoub MH, Yu-Chin Lin YC, Hao-Yang Lee HY, Lo CH, Khatib MM. Iranian ultrapotassic volcanism at ~11 Ma signifies the initiation of post-collisional magmatism in the Arabia–Eurasia collision zone. Terra Nova. 2013; 25:405-413.

16. Sorkhabi R. Tectonic Evolution, Collision, and Seismicity of Southwest Asia: In Honor of Manuel Berberian's Forty-Five Years of Research Contributions. Geol. Soc. Am. Spec. Pa. 2017;525.

17. Pang KN, Chung SL, Zarrinkoub MH, Khatib MM, Mohammadi SS, Chiu HY, Chu CH, Lee HY, Lo CL. Eocene–Oligocene post-collisional magmatism in the Lut Sistan region, eastern Iran: Magma genesis and tectonic

implications. Lithos. 2013;180-181:234-251.

18. Agard P, Omrani J, Jolivet L, Whitechurch H, Vrielynck B, Spakman W, Monié P, Meyer B, Wortel R. Zagros orogeny: a subduction-dominated process. Geol. Mag. 2011; 148:692-725.

19. Alavi M, Vaziri H, Seyed-Emami K, Lasemi Y. The Triassic and associated rocks of the Nakhlak and Aghdarband areas in central and northeastern Iran as remnants of the southern Turanian active continental margin. Geol. Soc. Am. Bul. 1997; 109:1563-1575.

20. McCall GJH. The geotectonic history of the Makran and adjacent areas of southern Iran. J. SE Asian Earth Sci. 1997; 15:517-531.

21. Tirrul R, Bell IR, Griffis RJ, Camp VE. The Sistan suture zone of eastern Iran. Geol. Soc. Am. Bull. 1983; 94:134-150.

22. Richards JP. Tectonic, magmatic, and metallogenic evolution of the Tethyan orogen: From subduction to collision. Ore Geol. Rev. 2015;323-345.

23. Ghafaribijar S. Geochemistry of Potassic Mafic Rocks in the Lar Complex, North of Zahedan, East of Iran. M.Sc. Thesis, Sistan and Baluchestan Univ. 2010.

24. Mohammadi A, Burg JP, Bouilhol P,Ruh J. U–Pb geochronology and geochemistry of Zahedan and Shah Kuh plutons, southeast Iran: Implication for closure of the South Sistan suture zone. Lithos. 2016;248-251:293-308.

25. Gittins J, Fawcett JJ, Brooks CK, Rucklidge JC. Intergrowths of nepheline-K-feldspar and kalsilite-K-feldspar: A reexamination of the pseudo-leucite problem. Contrib. Mineral. Petrol. 1980; 73:119-126.

26. Mitchell RH, Bergman SC. Petrology of lamproites. Plenum Press, New York, London. 1991;447.

27. Esperanca S, Holloway JR. The origin of high-K latites from Camp Creek, Arizona: constraints from experiments with variable fO_2 and H_2O. Contrib. Mineral. Petrol. 1986; 93:504-512.

28. Righter K, Carmichael ISE. Phase equilibria of phlogopite lamprophyres from western Mexico: biotite liquid equilibria and P–T estimates for biotite-bearing igneous rocks. Contrib. Mineral. Petrol. 1996; 123:1-21.

29. Kamenetsky VS, Elburg MA, Arculus R, Thomas R. Magmatic origin of low-Ca olivine in subduction-related magmas: co-existence of contrasting magmas. Chem. Geol. 2006; 233:346-357.

30. Ionov DA, Doucet LS, Ashchepkov IV. Composition of the lithospheric mantle in the Siberian craton: New constraints from fresh peridotites in the Udachnaya-East kimberlite. J. Petrol. 2010; 51:2177-2210.

31. Gavrilenko M, Herzberg C, Vidito C, Carr MJ, Travis Tenner T, Ozerov A. A calcium-in-olivine geohygrometer and its application to subduction zone magmatism. J. Petrol. 2016; 9:1811-1832.

32. Spandler C, O'Neill HSC. Diffusion and partition coefficients of minor and trace elementsinSanCarlosolivineat1300 1C with some geochemical implications. Contrib. Mineral. Petrol. 2010; 159:791-818.

33. Bussweiler Y, Foley SF, Prelević D, Jacob DE. The olivine macrocryst problem: New insights from minor and trace element compositions of olivine from Lac de Gras kimberlites, Canada. Lithos. 2015; 223:220-252.

34. Prelević D, Foley SF. Accretion of arc-oceanic lithospheric mantle in the Mediterranean: evidence from extremely high-Mg olivines and Cr-rich spinel inclusions in lamproites. Earth Planet. Sci. Lett. 2007; 256:120-135.

35. Sobolev NV, Logvinova AM, Zedgenizov DA, Pokhilenko NP, Malygina EV, Kuzmin DV, Sobolev AV. Petrogenetic significance of minor elements in olivines from diamonds and peridotite xenoliths from kimberlites of Yakutia. Lithos. 2009; 112:701-713.

36. Foley SF, Musselwhite DS, van der Laan SR. Melt compositions from ultramafic vein assemblages in the lithospheric mantle: a comparison of cratonic and non-cratonic settings. In: Gurney JJ, Gurney JL, Pascoe MD, Richardson SH, (eds) Proceedings of the 7th International Kimberlite Conference. Cape Town: Red Roof Design. 1999;238-246.

37. Tappe S, Foley SF, Jenner GA, Heaman LM, Kjarsgaard BA, Romer RL, Stracke A, Joyce N, Hoefs J. Genesis of ultramafic lamprophyres and carbonatites at Aillik Bay, Labrador: a consequence of incipient lithospheric thinning beneath the North Atlantic craton. J. Petrol. 2006; 47:1261-1315.

38. Tappe S, Foley SF, Kjarsgaard BA, Romer RL, Heaman LM, Stracke A, Jenner GA. Between carbonatite and lamproite—Diamondiferous Torngat ultramafic lamprophyres formed by carbonate-fluxed melting of cratonic MARID-type metasomes. Geochim. Cosmochim. Acta. 2008; 72:3258-3286.

39. Jaques AL, Green DH. Anhydrous melting of peridotite at 0–15 kb pressure and the genesis of tholeiitic basalts. Contrib. Mineral. Petrol. 1980; 73:287-310.

40. Rudnick RL, McDonough WF, Chappell BW. Carbonatite metasomatism in the northern Tanzanian mantle petrographic and geochemical characteristics. Earth Planet. Sci. Lett. 1993;114; 463-475.

41. Brett RC, Russell JK, Moss S. Origin of olivine in kimberlite: phenocryst or impostor? Lithos. 2009; 112:201-212.

42. Neumann ER, Wulff-Pedersen E, Simonsen SL, Pearson NJ, Marti J, Mitjavila J. Evidence for fractional crystallization of periodically refilled magma chambers in Tenerife, Canary Islands. J. Petrol. 1999; 40:1089-1123.

43. Prelević D, Foley SF, Romer RL, Conticelli S. Mediterranean Tertiary lamproites: multicomponent melts in postcollisional dynamics. Geochim. Cosmochim. Acta. 2008;72: 2125-2156.

44. Sobolev NV, Logvinova AM, Zedgenizov DA, Pokhilenko NP, Kuzmin DV, Sobolev AV. Olivine inclusions in Siberian diamonds: high-precision approach to minor elements. Eur. J. Mineral. 2008; 20:305-315.

45. Whitney DL, Evans BW. Abbreviations for Names of Rock-Forming Minerals. Am. Mineral. 2010;95(1):185-187.